

Communication

Scanning Rate Enhancement of Leaky-Wave Antennas Using Slow-Wave Substrate Integrated Waveguide Structure

Dong-Fang Guan¹, Qingfeng Zhang¹, Peng You¹, Zhang-Biao Yang, Yang Zhou, and Shao-Wei Yong

Abstract—In this communication, we propose a high scanning rate leaky-wave antenna (LWA) based on a slow-wave substrate integrated waveguide (SIW) structure. The slow-wave effect is introduced by etching periodical slots on the top surface of SIW. The LWA radiation is subsequently realized by introducing sinusoidal modulation to the slots profile. Such a structure significantly improves the scanning rate of LWA due to the small group velocity at the slow-wave region. Simulation and measured results indicate that the proposed LWA scans a wide angle in a narrow bandwidth near the cutoff frequency of surface plasmon polariton. Within the frequency band 13.5–13.9 GHz (3% relative bandwidth), the measured scanning angle is from 2° to 37° with the measured gain all above 9.2 dBi.

Index Terms—Leaky-wave antenna (LWA), scanning rate, slow wave, substrate integrated waveguide (SIW).

I. INTRODUCTION

Leaky-wave antennas (LWAs), supporting a traveling wave with continuous leakage along the structure, achieve high directivity with a simple feeding architecture [1]–[3]. No complicated and costly feed network is needed for LWAs, in contrast to the typical phased array. Recently, substrate integrated waveguide (SIW) LWAs have attracted much attention, due to the advantages of SIW, e.g., low profile, low cost, and easiness of integration with planar circuits [4], [5].

Generally, LWAs can be divided into two groups: uniform (or quasi-uniform) structure LWAs and periodic LWAs. In the first case, the structure supports a fast wave with respect to the free space, and hence, the phase constant of the leaky mode is smaller than that in free space. The fast-wave mode LWA is able to radiate directly [6]–[9]. In the second case, the guiding structure typically supports a slow wave with respect to the free space, and hence, the fundamental mode is a nonradiating mode. By introducing a periodic profile modulation along the guiding structure, the first-harmonic mode enters the fast-wave region and hence radiates [10], [11].

Scanning rate (scanning-range/bandwidth ratio), defined as the scanning angle range divided by the bandwidth, is a very important

parameter for frequency scanning antennas such as LWAs. For fixed-beam applications, one pursues that the antenna can operate over a wide bandwidth with consistent radiation performance. While for scanning-beam applications, one requires a high scanning rate, which reduces the required bandwidth (for the same scanning range) and hence eases the transceiver architecture and signal processor from the system viewpoint. However, very few works were reported so to discuss how to enhance the scanning rate of LWAs. Actually, most reported LWAs need a large bandwidth to operate beam scanning. It is difficult to design the RF transceivers for such antennas. Therefore, it is highly demanded to increase the scanning rate and hence reduce the bandwidth of LWAs without sacrificing the beam scanning capability. A novel composite right/left handed-SIW LWA was proposed in [12] to achieve a wide continuous scanning range within a relatively narrow fractional bandwidth. However, the bandwidth is still as large as 26%, due to the fact that it works in the fast-wave region. Employing slow-wave structure is a potential way to improve scanning rate of LWAs, because the phase constant of a slow wave is much more sensitive to frequency variations [13]–[15]. By introducing meandering line to SIW LWA, one realizes an equivalent slow-wave transmission line (TL) and hence improves the scanning rate, but with the price of increasing the lateral size [15]. Some other slow-wave SIWs are realized by adding several rows of metallic blind holes [16], [17] or patterning with microstrip polyines [18], which are, however, difficult to form LWA due to the complicated structures. Researchers also explored some slow-wave structures based on parallel plate waveguide [19] or microstrip line [20]. In comparison, SIW exhibit better shielding performance and hence provide a good isolation between adjacent feeding lines.

In this communication, we propose a high scanning rate LWA based on a novel slow-wave SIW TL. By etching periodic slots on the top surface of the SIW, slow-wave effect is introduced to SIW TL. We subsequently modulate the slot profile to allow the first space harmonic to radiate and hence form an LWA. To enhance the scanning rate, we intentionally employ the frequency band near the upper cutoff frequency for radiation, because the phase constant is very sensitive to frequency variation within this range. In the operating band of 13.5–13.9 GHz, the designed LWA has a scanning range of 2°–37° with the radiation gain above 9.2 dBi. The relative scanning bandwidth is only 3%.

This communication is organized as follows. The configuration and analysis of the slow-wave SIW are first presented in Section II, followed by the LWA design in Section III and the experimental validation in Section IV. Conclusion is finally given in Section V.

II. PRINCIPLE OF SLOW-WAVE SIW TL

Fig. 1 is the configuration of the proposed slow-wave SIW TL. It is designed on the Rogers RT 5880 printed circuit board with thickness $h = 0.508$, relative dielectric constant $\epsilon_r = 2.2$, and loss tangent $\tan\delta = 0.001$. Periodical slots are etched on the top surface of SIW to form slow-wave effect. The width of SIW is w_s .

Manuscript received November 14, 2017; revised February 7, 2018; accepted April 8, 2018. Date of publication April 30, 2018; date of current version July 3, 2018. This work was supported in part by the Natural Science Foundation of Hunan Province, China, under Grant 2017JJ3364, in part by the National Natural Science Foundation of China under Grant 61601487, in part by Guangdong Natural Science Funds for Distinguished Young Scholar under Grant 2015A030306032, in part by the Talent Support Project of Guangdong under Grant 2016TQ03X839, in part by Shenzhen Science and Technology Innovation Committee Funds under Grant KQJSCX20160226193445, Grant KQCX2015033110182368, Grant JC YJ20160301113918121, and Grant JSGG20160427105120572, and in part by Shenzhen Development and Reform Commission Funds under Grant [2015] 944. (Corresponding author: Qingfeng Zhang.)

D.-F. Guan, P. You, Z.-B. Yang, Y. Zhou, and S.-W. Yong are with the College of Electronic Science and Engineering, National University of Defense Technology, Changsha 410073, China (e-mail: gdfguandongfang@163.com).

Q. Zhang is with the Department of Electronics and Electrical Engineering, Southern University of Science and Technology, Shenzhen 518055, China (e-mail: zhang.qf@sustc.edu.cn).

Color versions of one or more of the figures in this communication are available online at <http://ieeexplore.ieee.org>.

Digital Object Identifier 10.1109/TAP.2018.2831257

0018-926X © 2018 IEEE. Personal use is permitted, but republication/redistribution requires IEEE permission.

See http://www.ieee.org/publications_standards/publications/rights/index.html for more information.

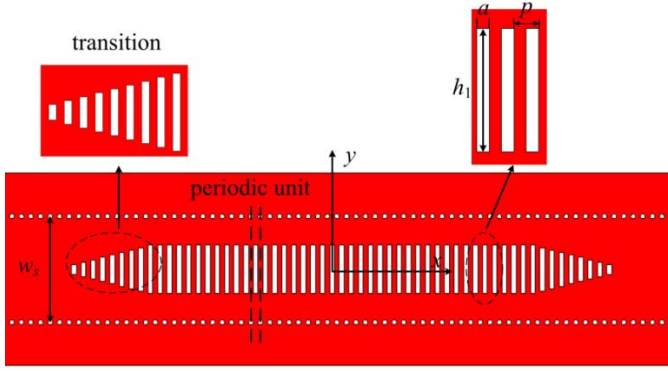


Fig. 1. Configuration of the proposed slow-wave SIW TL.

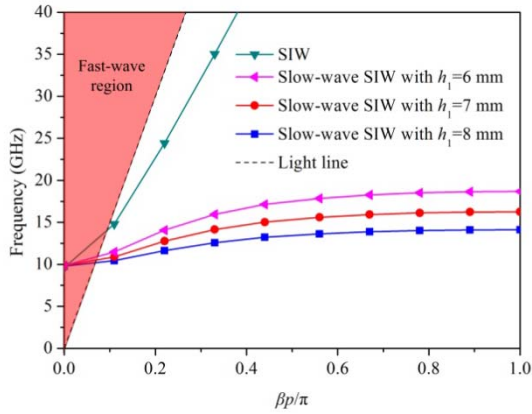


Fig. 2. Dispersion curve of the periodic unit.

The period of the slots is p . The width and length of slots are a and h_1 , respectively. To propagate a slow-wave mode at microwave frequencies, the parameters a and p are set much less than the guided wavelength at the operational frequency. As shown in Fig. 1, a smooth transition section, in which the slot length varies from $0.2 h_1$ to h_1 with a linear gradient, is employed to realize a good impedance matching.

In our previous work [17], slow-wave effect is realized in SIW by employing arrays of transverse metallic blind holes, which requires a thick substrate for digging blind via holes and needs a very complicated fabrication. In contrast, the proposed novel slow-wave TL is realized by etching slots on the surface of SIW, which features simplicity in fabrication and compactness in thickness. Moreover, this structure can be designed as an LWA by directly introducing sinusoidal modulation to the slot length, which will be introduced in Section III. The dispersion characteristic of the proposed slow-wave TL is analyzed using commercial EM software CST under the Eigen mode analysis, in which one periodic unit (including the lateral vias) as shown in Fig. 1 is modeled to obtain the dispersion curve. The parameters are fixed as: $w_s = 11$ mm, $a = 0.5$ mm, $p = 1$ mm. Fig. 2 shows the simulated dispersion curves of a pure SIW and slow-wave SIW with different slot length h_1 for comparison. It can be seen that the slow-wave SIW structure has the same lower cutoff frequency as SIW. As β increases, the slopes of slow-wave SIW curves decrease gradually and the slow-wave feature emerges. Note that, the slow-wave SIW has an upper cutoff frequency which is inversely proportional to the slot length h_1 . The dispersion curve indicates that the proposed slow-wave SIW structure has fast-wave feature at low frequencies and slow-wave feature at high frequencies.

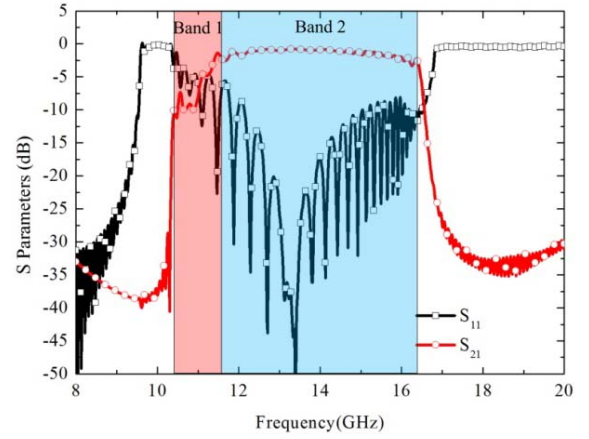


Fig. 3. Transmission characteristic of the proposed slow-wave SIW TL.

Thus it can support a hybrid fast-wave and slow-wave modes at different frequencies.

Fig. 3 shows the simulated reflection coefficient (S_{11}) and transmission coefficient (S_{21}) of the proposed slow-wave SIW TL. The slot length is set as 7 mm in the simulation. The passband is from 10.3 to 16.3 GHz, which agrees well with the dispersion feature shown in Fig. 2. According to Fig. 2, the proposed TL has both fast-wave (leaky-wave mode) and slow-wave bands, which correspond to Band 1 and Band 2 of Fig. 3, respectively. In the fast-wave region Band 1, the propagation constant β is smaller than the wavenumber in free space k_0 . The angle of maximum radiation direction from the broadside (θ) of LWA can be determined as

$$\sin \theta = \frac{\beta}{k_0}. \quad (1)$$

The Band 1 in Fig. 3 corresponds to this leaky wave mode and the energy directly radiates out through the slots. The corresponding beam scanning angle is only limited to the forward direction. Actually, most SIW LWAs with transverse slots work in this fast-wave region [6]–[8]. The Band 2 in Fig. 3 is the slow-wave region, in which the propagation constant β is larger than k_0 . This mode is nonradiating and the energy is mostly transmitted to terminal port. Thus Band 2 can be seen as a transmission mode. As shown in Fig. 3, the loss of the proposed slow-wave TL is 0.7 dB at the transmission center frequency 13.5 GHz. The propagation constant of slow-wave SIW is much larger than that of SIW, especially as the frequency goes close to the upper cutoff frequency. Moreover, β is more sensitive to the variation of frequency in the case of slow-wave SIW, according to Fig. 2. Therefore, according to formula (1), the LWA based on such a structure is potentially a high scanning rate antenna. To maximize the scanning rate, we may choose the band near the upper cutoff frequency, where β changes quickly with the frequency.

III. LWA BASED ON SLOW-WAVE SIW TL

Periodic profile modulation introduces infinite space harmonics, whose phase constant β_n is calculated as

$$\beta_n = \beta + \frac{2\pi n}{d}, \quad n = 0, \pm 1, \pm 2, \dots \quad (2)$$

where d is the modulation period. The $n = -1$ space harmonic is usually chosen to convert transmission wave to radiation wave. In this mode, the LWA can scan beam in either the forward direction or the backward direction.

The configuration of the proposed LWA based on the slow-wave SIW TL is shown in Fig. 4, in which sinusoidal modulation is

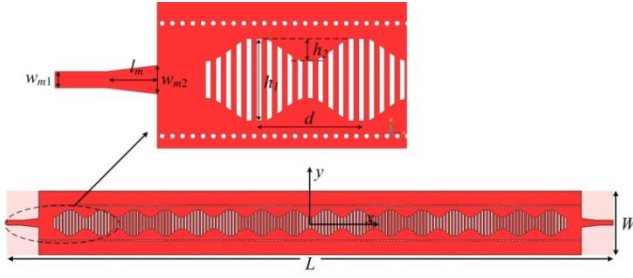


Fig. 4. Configuration of the sinusoidally modulated LWA based on slow-wave SIW TL.

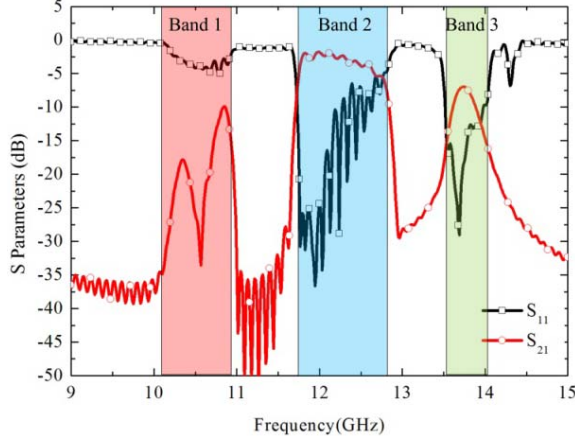


Fig. 5. S-parameters of the sinusoidally modulated LWA.

introduced to excite the $n = -1$ space harmonic wave. The antenna size $L \times W$ is $190 \text{ mm} \times 20 \text{ mm}$. The amplitude of the sinusoidal modulation is $h_2/2$. It means that the maximum and the minimum slot lengths are h_1 and $h_1 - h_2$, respectively. The modulated period d is set as one guided wavelength (slow-wave SIW) at the broadside frequency f_0 . According to formulas (1) and (2), β_{-1} is zero at f_0 and the radiation direction is at broadside in this case. When the operating frequency $f < f_0$, β_{-1} is negative and the scanning beam is in the backward direction. When the operating frequency $f > f_0$, β_{-1} is positive and the scanning beam is in the forward direction. To increase the scanning rate of the proposed LWA, the operating frequency is set close to the upper cutoff frequency f_c , and only the frequency band $f_0 < f < f_c$ is used. Here, we choose $h_1 = 8 \text{ mm}$, $h_2 = 2.2 \text{ mm}$, and $d = 10.1 \text{ mm}$, which corresponds to a broadside frequency (f_0) close to 13.2 GHz . We use 16 modulation periods in our design to radiate out most of the energy. For measurement convenience, SIW is finally connected to a microstrip line using a transition. As shown in Fig. 4, the width of the 50Ω microstrip line is w_{m1} . The width and length of the tapered microstrip lines are w_{m2} and l_m for impedance matching. The final parameters are $w_{m1} = 1.6 \text{ mm}$, $w_{m2} = 2.8 \text{ mm}$, and $l_m = 5 \text{ mm}$.

Fig. 5 shows the simulated S-parameters of the sinusoidally modulated LWA. It can be seen from Fig. 5 that there are three radiating bands. Band 1 corresponds to the direct radiation through the slots by the fast-wave waveguide mode, since this frequency range is the same as the original Band 1 in Fig. 3. According to formula (1), Band 1 is in the region from the SIW cutoff frequency to the frequency at $\beta = k_0$, and the beam radiates in the forward direction. Band 2 and Band 3 correspond to $n = -1$ space harmonic due to the slot profile modulation. Ideally, Band 2 and Band 3 are connected together to form the forward and backward radiation regions. However, an open stopband occurs around the broadside frequency due to the symmetric



Fig. 6. Photograph of the proposed sinusoidally modulated LWA.

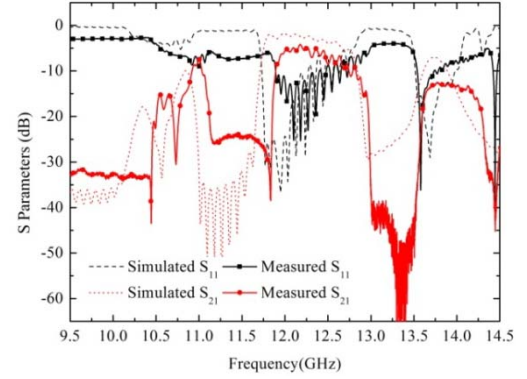


Fig. 7. Measured and simulated reflection coefficients (S_{11}) and transmission coefficients (S_{21}) of the sinusoidally modulated LWA.

profile used in the modulation. Therefore, the original $n = -1$ space harmonic splits into two separate frequency bands, i.e., Band 2 and Band 3, corresponding to backward and forward radiation, respectively. The space between Band 2 and Band 3 corresponds to the open stopband around the broadside radiation. This open stopband around the broadside radiation is a common problem in LWA. One may overcome it by using asymmetric structures, as did in [21] and [22]. We will explore this improvement in our future works. Considering the scanning rate, Band 3 is the desired band since it is closer to the upper cutoff frequency.

IV. EXPERIMENTAL VALIDATION AND DISCUSSION

To validate the above analysis, the proposed slow-wave SIW LWA is fabricated and measured. A fabricated prototype is shown in Fig. 6. The simulated and measured reflection and transmission coefficients are shown in Fig. 7. It can be seen from Fig. 7 that the trend of the measured curves is accordant with the simulated ones. The loss (S_{21}) of the measurement result is a bit higher than the simulated one.

This loss difference is mainly resulted from the material tolerance and sharp slot corners and thin metal that are difficult to be accurately meshed in simulations. In addition, the connectors and weld also introduce more losses. In the desired Band 3, the measured S_{21} is below -13 dB and S_{11} is below -7 dB , which indicates that most energy is radiated out by the modulated slots. The antenna radiation patterns are measured in a chamber with a far-field setup from 13.5 to 13.9 GHz . The measured and simulated radiation patterns are plotted in Fig. 8. A more detailed comparison between simulated and measured radiation performance is listed in Table I. It can be seen that the simulated beam angle is scanned from 2° to 39° within the frequency band from 13.5 to 13.9 GHz , while the measured scanning angle is scanned from 2° to 37° . Therefore, the antenna has a scanning range of 35° in a narrow bandwidth of only 3% (400 MHz). All the measured sidelobe levels (SLLs) are below -8.3 dB . The simulated gain reaches up to 10 – 14.2 dBi , while the measured gain is within

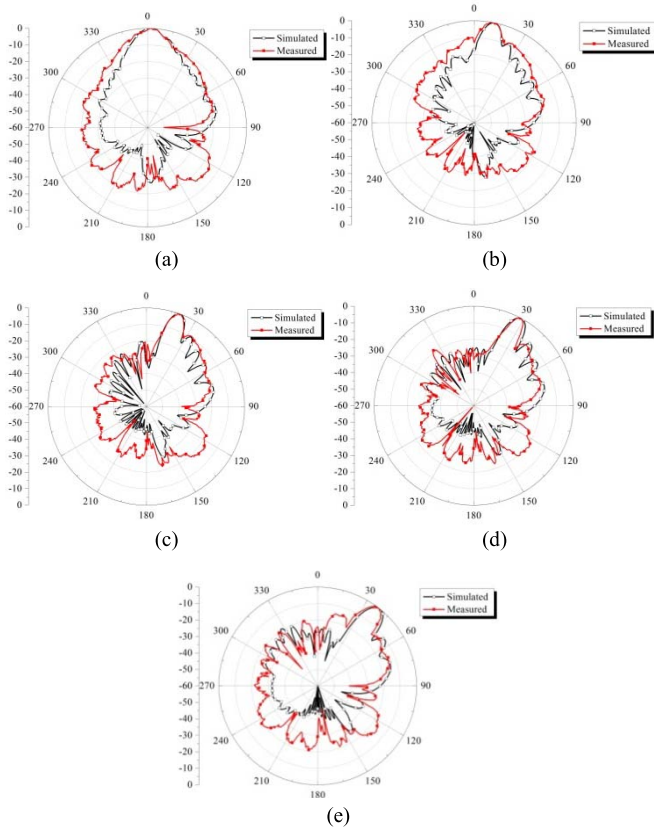


Fig. 8. Measured and simulated radiation patterns of the sinusoidally modulated LWA at (a) 13.5, (b) 13.6, (c) 13.7, (d) 13.8, and (e) 13.9 GHz.

TABLE I
SIMULATION AND MEASURED RESULTS COMPARISON

Frequency (GHz)	Beam Direction (degree)		SLL (dB)		Gain (dBi)	
	Sim.	Mea.	Sim.	Mea.	Sim.	Mea.
13.5	2	2	-17.1	-14.8	11.7	11.1
13.6	12	11	-9.4	-8.3	14.2	13.3
13.7	20	20	-9.7	-9.2	13.9	12.2
13.8	29	28	-9.3	-11.8	12.3	11.5
13.9	39	37	-10.6	-13.9	10	9.2

TABLE II
PERFORMANCE COMPARISON OF DIFFERENT SIW LWAs

	Center frequency (GHz)	Scanning range (degree)	Bandwidth (%)	Scanning Rate	Type
[7]	11	60	16.4	3.7	SIW with slots
[12]	9.55	119	26.2	4.5	SIW-CRLH
[15]	25.25	50	9.9	5.1	Meandering SIW
This work	13.7	35	3	11.7	slow-wave SIW

the range of 9.2–13.3 dBi. The discrepancy between the simulation and measured results is mainly due to the higher losses brought by the connectors and practical materials.

The major contribution of this communication lies in that the proposed antenna has a large scanning rate or equivalently beam

scanning range/bandwidth ratio. To better show this, we compare it with other representative SIW LWAs in Table II. Here, we define the scanning rate as the scanning angle per 1% relative bandwidth. In our design, the angle scanning range is 35° and the relative bandwidth is 3%, so the scanning rate is 11.7, which means that the beam scans 11.7° within 1% relative bandwidth. It can be seen from Table II that the scanning rate of the proposed antenna is the highest and is almost twice more than other LWAs.

V. CONCLUSION

In this communication, we have proposed a slow-wave SIW LWA for high scanning rate radiations. A novel slow-wave SIW transmission line was designed and analyzed. It revealed that the proposed structure had the fast-wave feature and slow-wave feature at different bands. By introducing sinusoidal modulation to the slow-wave TL, one designed an LWA. In the slow-wave region near the upper cutoff frequency, the proposed antenna exhibited a high scanning rate of 11.7, i.e., scanning 35° range within only 3% relative bandwidth. Compared with other SIW LWAs, the proposed antenna featured the highest scanning rate.

REFERENCES

- [1] D. R. Jackson, A. A. Oliner, and C. Balanis, *Modern Antenna Handbook*. Hoboken, NJ, USA: Wiley, 2008.
- [2] F. Monticone and A. Alù, "Leaky-wave theory, techniques, and applications: From microwaves to visible frequencies," *Proc. IEEE*, vol. 103, no. 5, pp. 793–821, May 2015.
- [3] D. R. Jackson, C. Caloz, and T. Itoh, "Leaky-wave antennas," *Proc. IEEE*, vol. 100, no. 7, pp. 2194–2206, Jul. 2012.
- [4] D. Deslandes and K. Wu, "Substrate integrated waveguide leaky-wave antenna: Concept and design considerations," in *Proc. Asia-Pacific Microw. Conf.*, Dec. 2005, pp. 346–349.
- [5] D.-F. Guan, C. Ding, Z.-P. Qian, Y.-S. Zhang, Y. J. Guo, and K. Gong, "Broadband high-gain SIW cavity-backed circular-polarized array antenna," *IEEE Trans. Antennas Propag.*, vol. 64, no. 4, pp. 1493–1497, Apr. 2016.
- [6] J. Liu, D. R. Jackson, and Y. Long, "Substrate integrated waveguide (SIW) leaky-wave antenna with transverse slots," *IEEE Trans. Antennas Propag.*, vol. 60, no. 1, pp. 20–29, Jan. 2012.
- [7] J. Liu, X. Tang, Y. Li, and Y. Long, "Substrate integrated waveguide leaky-wave antenna with H-shaped slots," *IEEE Trans. Antennas Propag.*, vol. 60, no. 8, pp. 3962–3967, Aug. 2012.
- [8] J. Liu, D. R. Jackson, Y. Li, C. Zhang, and Y. Long, "Investigations of SIW leaky-wave antenna for endfire-radiation with narrow beam and sidelobe suppression," *IEEE Trans. Antennas Propag.*, vol. 62, no. 9, pp. 4489–4497, Sep. 2014.
- [9] A. Mallahzadeh and S. Mohammad-Ali-Nezhad, "Long slot ridged SIW leaky wave antenna design using transverse equivalent technique," *IEEE Trans. Antennas Propag.*, vol. 62, no. 11, pp. 5445–5452, Nov. 2014.
- [10] X. Bai, S.-W. Qu, K.-B. Ng, and C. H. Chan, "Sinusoidally modulated leaky-wave antenna for millimeter-wave application," *IEEE Trans. Antennas Propag.*, vol. 64, no. 3, pp. 849–855, Mar. 2016.
- [11] A. J. Martinez-Ros, J. L. Gómez-Tornero, V. Losada, F. Mesa, and F. Medina, "Non-uniform sinusoidally modulated half-mode leaky wave lines for near-field focusing pattern synthesis," *IEEE Trans. Antennas Propag.*, vol. 63, no. 3, pp. 1022–1031, Mar. 2015.
- [12] Q. Yang, Y. Zhang, and X. Zhang, "X-band composite right/left-handed leaky wave antenna with large beam scanning-range/bandwidth ratio," *Electron. Lett.*, vol. 48, no. 13, pp. 746–747, Jun. 2012.
- [13] D.-F. Guan, P. You, Q. Zhang, Z.-H. Lu, S.-W. Yong, and K. Xiao, "A wide-angle and circularly polarized beam-scanning antenna based on microstrip spoof surface plasmon polariton transmission line," *IEEE Antennas Wireless Propag. Lett.*, vol. 16, pp. 2538–2541, 2017.
- [14] Y. Geng, J. Wang, Y. Li, Z. Li, M. Chen, and Z. Zhang, "Leaky-wave antenna array with a power-recycling feeding network for radiation efficiency improvement," *IEEE Trans. Antennas Propag.*, vol. 65, no. 5, pp. 2689–2694, May 2017.

- [15] W. Cao, W. Hong, Z. N. Chen, B. Zhang, and A. Liu, "Gain enhancement of beam scanning substrate integrated waveguide slot array antennas using a phase-correcting grating cover," *IEEE Trans. Antennas Propag.*, vol. 62, no. 9, pp. 4584–4591, Sep. 2014.
- [16] A. Niembro-Martín *et al.*, "Slow-wave substrate integrated waveguide," *IEEE Trans. Microw. Theory Techn.*, vol. 62, no. 8, pp. 1625–1633, Aug. 2014.
- [17] D.-F. Guan, P. You, Q. Zhang, K. Xiao, and S.-W. Yong, "Hybrid spoof surface plasmon polariton and substrate integrated waveguide transmission line and its application in filter," *IEEE Trans. Microw. Theory Techn.*, vol. 65, no. 12, pp. 4925–4932, Dec. 2017.
- [18] H. Jin, K. Wang, J. Guo, S. Ding, and K. Wu, "Slow-wave effect of substrate integrated waveguide patterned with microstrip polyline," *IEEE Trans. Microw. Theory Techn.*, vol. 64, no. 6, pp. 1717–1726, Jun. 2016.
- [19] S. C. Pavone, E. Martini, F. Caminita, M. Albani, and S. Maci, "Surface wave dispersion for a tunable grounded liquid crystal substrate without and with metasurface on top," *IEEE Trans. Antennas Propag.*, vol. 65, no. 7, pp. 3540–3548, Jul. 2017.
- [20] D. R. Smith, O. Yurduseven, L. P. Mancera, and P. Bowen, "Analysis of a waveguide-fed metasurface antenna," *Phys. Rev. Appl.*, vol. 8, no. 5, p. 054048, 2017.
- [21] S. Otto, A. Al-Bassam, A. Rennings, K. Solbach, and C. Caloz, "Radiation efficiency of longitudinally symmetric and asymmetric periodic leaky-wave antennas," *IEEE Antennas Wirel. Propag. Lett.*, vol. 11, pp. 612–615, Jun. 2012.
- [22] X.-L. Tang *et al.*, "Continuous beam steering through broadside using asymmetrically modulated goubau line leaky-wave antennas," *Sci. Rep.*, vol. 7, Sep. 2017, Art. no. 11685.